



# InGaN-LD-pumped $\text{Pr}^{3+}:\text{LiYF}_4$ continuous-wave deep red lasers at 697.6 and 695.8 nm



Bin Xu<sup>a</sup>, Yongjie Cheng<sup>a</sup>, Biao Qu<sup>a</sup>, Saiyu Luo<sup>a</sup>, Huiying Xu<sup>a</sup>, Zhiping Cai<sup>a,\*</sup>, Patrice Camy<sup>b</sup>, Jean-Louis Doualan<sup>b</sup>, Richard Moncorgé<sup>a,b</sup>

<sup>a</sup> Department of Electronic Engineering, Xiamen University, Xiamen 361005, People's Republic of China

<sup>b</sup> Centre de Recherche sur les Ions, les Matériaux et la Photonique (CIMAP), UMR 6252 CEA-CNRS-ENSICAEN, Université de Caen, 14050 Caen, France

## ARTICLE INFO

### Article history:

Received 6 August 2014

Received in revised form

24 September 2014

Accepted 14 October 2014

Available online 6 November 2014

### Keywords:

Pr:YLF crystal

Power scaling

Deep red lasers

## ABSTRACT

We report a power-scaled operation at  $\pi$ -polarized  $\sim 698$  nm and  $\sigma$ -polarized  $\sim 696$  nm deep red lasers in Pr:YLF crystal pumped by a 2-W InGaN LD (laser diode) after a pump beam reshaping. The maximum output power of the  $\pi$ -polarized laser emission at 697.6 nm was up to 348 mW with slope efficiency of about 32.7% in a free-running mode. The  $\sigma$ -polarized laser emission at 695.8 nm was also realized for the first time using a simple and compact Brewster-angle orientated intracavity etalon playing role as birefringence filter and the generated maximum output power of the 695.8 nm laser was up to 116 mW with slope efficiency of about 18.5% with respect to the absorbed pump power.

© 2014 Elsevier Ltd. All rights reserved.

## 1. Introduction

In recent years, owing to an energy level scheme that enables several transitions in the red, orange, green, or blue spectral region, trivalent praseodymium ( $\text{Pr}^{3+}$ ) doped laser materials are of great interest for obtaining laser emissions in the visible spectrum. These visible lasers could be very desirable in the development of color displays, micro-sized projectors, and holographic and lithographic techniques, as well as in biomedical or quantum optical applications. In order to achieve these visible lasers, the  $\text{Pr}^{3+}$  ions need to be pumped from  $^3\text{H}_4$  ground level to  $^3\text{P}_0$  (around 480 nm),  $^3\text{P}_1+^1\text{I}_6$  (around 469 nm), or  $^3\text{P}_2$  (around 444 nm) excited energy level. As a result, three pump sources have been developed to realize pumping of various  $\text{Pr}^{3+}$ -doped materials effectively. For example, OPSSL (optically pumped and frequency-doubled semiconductor lasers) at  $\sim 480$  nm [1], a diode-pumped and frequency-doubled Nd:YAG at  $\sim 469$  nm [2,3], and InGaN laser diodes at  $\sim 444$  nm [4–6]. Among them, the OPSSL is quite attractive because of its advantages, such as good beam quality, high output power and favorable emitting wavelength at 480 nm matching with the maximum absorption of some  $\text{Pr}^{3+}$ -doped materials, especially Pr:YLF ( $\text{LiYF}_4$ ) crystal. However, the extra-high price prohibits its practicability as a pump source. So far, the most commonly used ones are the InGaN laser diodes, mainly because of their compactness, commercial availability and acceptable price.

The InGaN laser diodes can provide blue laser from 440 nm to 450 nm with maximum output power now to 2 W and more important with polarized emitting, which satisfies the requirement of polarization-dependent absorption of some  $\text{Pr}^{3+}$ -doped anisotropic crystals, such as uniaxial YLF, LLF ( $\text{LiLuF}_4$ ) and Pr:KYF<sub>4</sub>, as well as biaxial crystal BYF ( $\text{BaY}_2\text{F}_8$ ). On the other hand, an important property of fluoride materials is their low non-radiative decay rates, lower than oxides since the phonon energy of fluorides is lower than that of oxides. This has several positive effects on the performance of rare-earth-doped fluorides: (1) rare-earth-doped fluorides are generally more efficient luminescent systems; (2) less heat is dissipated in the fluoride crystal as a result of lower non-radiative rates; (3) as a result of the low non-radiative losses in fluorides, rare-earth-doped fluorides exhibit longer fluorescence lifetime of the emitting level than the rare-earth-doped oxides. Among  $\text{Pr}^{3+}$  doped fluoride hosts, Pr:YLF has absorbed considerable attention since its relatively high upper energy level fluorescence lifetime, which is of benefit to population inversion. Moreover, Pr:YLF has specific spectroscopic characteristics including plenty of emissions in visible region and some of them could be used for particular applications, e.g. a frequency-stabilized lasing line at 698 nm is a key component for the construction of the optical frequency standards based on strontium atoms [7]. Recently, using an InGaN laser diode pump source with nominal output power of 1 W, we demonstrated a diode-pumped Pr:YLF deep red laser at 698 nm [8] with maximum output power up to 156 mW. After this investigation, we improved the output power further to 215 mW [9] by optimizing the laser operation. Based on the 698 nm laser, we very recently obtained

\* Corresponding author.

E-mail address: [zpcai@xmu.edu.cn](mailto:zpcai@xmu.edu.cn) (Z. Cai).

lasing at  $\sigma$ -polarized 695.8 nm using a 7-mm-long BBO as birefringence filter [10]. The maximum output power at this emission was 51 mW with slope efficiency of 12.6%.

It is worthwhile to mention that at present among reports on  $\text{Pr}^{3+}$ -based lasers using InGaN as pump source, 1-W such laser diodes have been widely used. Clearly, a higher pump power is advantageous for power scaling to higher output power. In this paper, we proposed to use a 2-W InGaN laser diode as pump source of Pr:YLF lasers at the  $\pi$ -polarized 698 nm and the  $\sigma$ -polarized  $\sim$ 696 nm in order to achieve power scalabilities at both lasing wavelengths. Moreover, to obtain the  $\sigma$ -polarized  $\sim$ 696 nm laser, we employed an efficient and simple intracavity polarized beam selector, i.e. a Brewster-angle-orientated thin glass plate acting as birefringence filter instead of BBO birefringence filter to suppress the  $\pi$ -polarized 698 nm lasing. The pump beam was firstly reshaped to optimize the pump beam quality. Thus, a maximum output power of the  $\pi$ -polarized laser emission at 697.6 nm was up to 348 mW with slope efficiency of about 32.7% and the maximum output power of the  $\sigma$ -polarized laser emission at 695.8 nm was 116 mW with slope efficiency of about 18.5%.

## 2. Experimental setup

The schematic experimental setup is shown in Fig. 1. The pump source is a commercially available InGaN blue laser diode with maximum output power of about 2 W. Such laser diodes with output power more than 500 mW usually have relatively bad beam quality characterized as non-circular beam spot [11] and multimode output beam [12]. The 2-W laser diode itself was integrated firstly with an aspheric lens (focal length  $f=3$  mm) for collimating the pump beam and then with a pair of cylindrical lenses ( $f=40$  and  $-8$  mm) for correcting the astigmatism of the pump beam. We checked the beam quality of the laser diode by recording its intensity profile using a CCD camera shown in Fig. 1, which shows a clear multimode in  $x$  direction with four split stripes. The emitting peak wavelengths of the pumping laser diode vary from 442 nm to 445.2 nm as the drive current change from about 0.12 A (threshold) to maximum of 1.32 A. The peak pumping wavelength is about 444 nm when the drive current was set at 1 A, which shows a good agreement with absorption of the laser crystal. The pump beam was focused into the laser crystal using an achromatic doublet lens with  $f=50$  mm, which has been found having better laser performance in contrast to coupling lens with  $f=40$  and 75 mm in our laser configuration. The laser resonator was a typically near-hemispherical cavity.

The coatings of the IM (input mirror) and OC (output coupler) used in this experiments were designed and fabricated in our lab by using plasma direct-current sputtering technology, which is also shown in Fig. 1. The flat dichroic IM has a maximum transmission at the 444 nm pump wavelength and is highly reflective (99.95%) for the deep red emissions. One OC was employed with transmissions of 0.92% at 696 nm and 0.85% at 698 nm. For suppressing laser emission at 640 nm which has higher emission cross section as  $2.23 \times 10^{-19} \text{ cm}^2$  than the investigated 698 and 696 nm lasers as  $5.63 \times 10^{-20} \text{ cm}^2$  and  $1.62 \times 10^{-20} \text{ cm}^2$ , respectively (see Fig. 2), the OC was coated with high transmissivity as more than 86% at 640 nm. In addition, the OC has radius of curvature of 50 mm. The laser crystal was a nicely polished but uncoated Pr:YLF with doping concentration of 0.5at% and thickness of 5 mm. The absorption ratios were measured from 47.2% to 82.8% due to the shift of the pump wavelengths at different drive current. A 0.1-mm intracavity glass etalon was inserted after the laser crystal acting as birefringence filter in order to suppress the  $\sim$ 698 nm lasing and in favor of  $\sim$ 696 nm lasing.

## 3. Results and discussion

It should be pointed out firstly that  $\text{Pr}^{3+}$  doped laser gain medium are generally very sensitive to the contribution of the

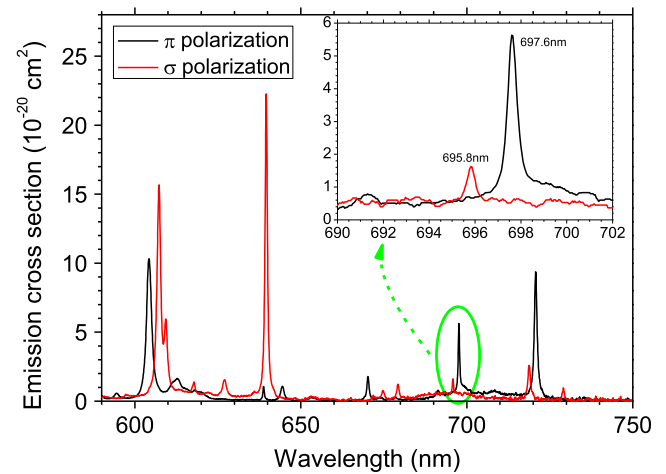


Fig. 2. Polarization-dependent emission cross sections of a Pr:YLF crystal. The inset shows the details of the investigated emission spectrum.

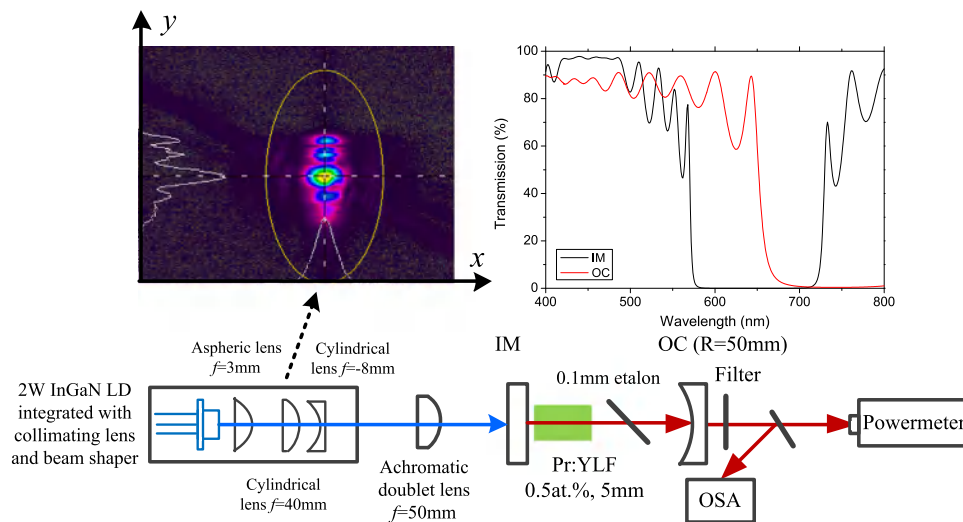


Fig. 1. Schematic experimental setup of a 2-W InGaN-LD-pumped Pr:YLF deep red lasers at 697.6 and 695.8 nm.

non-radiative cross relaxation processes [13,14] and multi-phonon decay to  $^1D_2$  energy level [13], which lead to reduction of upper-state lifetime and finally result in degradation of laser performance. Thus, in order to decrease the probability of these negative factors, a relatively weakly doped Pr:YLF laser crystal is required with 0.5at% doping concentration in this work.

A free-running operation was firstly demonstrated without inserting any other components inside the laser cavity except the Pr:YLF laser crystal. A power scaling to 348 mW was addressed with slope efficiency of about 32.7% with respect to absorbed pump power (see Fig. 3). Although the emission at about 720 nm ( $^3P_0 \rightarrow ^3F_4$  transition) has a 1.6 times higher emission cross section than that of 698 nm ( $^3P_0 \rightarrow ^3F_3$  transition), no lasing at  $\sim 720$  nm was observed in this experiment thanks to the relatively high total transmission as more than 4% (IM 3.7% and OC 0.45%). The absorbed threshold pump power was as low as 52 mW.

We very recently obtained lasing at  $\sigma$ -polarized 695.8 nm using a 7-mm-long BBO as birefringence filter [10]. The maximum output power at this emission was 51 mW with slope efficiency of 12.6%. In the period of that experiment, we tried 695.8 nm lasing by inserting a Brewster plate into the resonator.

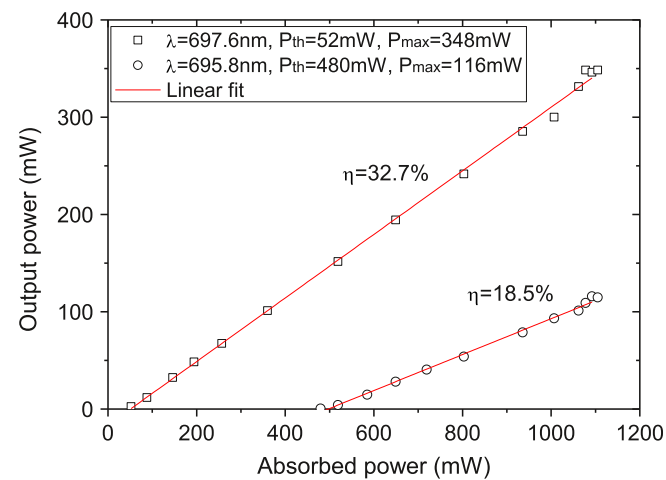


Fig. 3. The output power characteristics of the Pr:YLF crystal at 697.6 and 695.8 nm.

However, lasing at 640 nm in the same  $\sigma$  polarization was observed instead of 695.8 nm lasing, which should be explained as an inadequate coating design for the suppression of the 640 nm transition. In this work, the newly coated output mirror has a transmission at 640 nm of more than 86%, which is proved to be enough for suppressing the 640 nm lasing. Laser emission at 695.8 nm was obtained by inserting a 0.1-mm glass etalon into the laser cavity at Brewster angle just after the laser crystal instead of the less used BBO functioned as birefringent crystal. With respect to the specific 695.8 nm polarized lasing wavelength, the 0.1-mm Brewster-angle-placed glass etalon has an FSR of about 1822 GHz corresponding to about 2.9 nm, i.e. about 1.6 times of the space between 697.6 and 695.8 nm. This indicates the 695.8 nm has a high transmission while 697.6 nm locates at the lowest region of the transmission curve of the glass etalon. Finally, by finely adjusting the glass etalon to an optimized orientation and location, we realized the 695.8 nm laser emission with maximum output power up to 116 mW and slope efficiency of about 18.5% (see Fig. 3). Thus, this work represents an effective scaling of slope efficiency to the highest at present for this laser emission in Pr:YLF crystal. During the laser experiment, we kept the orientation of the glass etalon and moved it perpendicularly to the laser axis, and we found the laser cavity cannot always keep the same output amount. The laser result was changeable a little bit or to a great extent depending on the actual locations onto the glass etalon. This, in fact, could be the reflection of non-homogeneity of the glass etalon. In addition, we also found the laser result can be reproducible if only the laser cavity including the glass etalon was unmoved. We believe the current laser results can be further improved including the output powers and slope efficiencies by optimizing the doping concentration, the length and the quality of the laser crystal, as well as the output coupling.

Stable laser output is always desirable for various applications. The output power stabilities of the 697.6 and 695.8 nm lasers can be readily estimated by registering the instantaneous values of the output powers with time. Thus, the stabilities of the maximum output powers for the 697.6 and 695.8 nm lasers were deduced to be about 0.72% and 0.91% (RMS, root mean square), respectively.

The laser spectrum of single lasing wavelength at 697.6 and 695.8 nm was registered separately in Fig. 4 by using an Advantest Q8384 optical spectrum analyzer with resolution of about 0.1 nm.

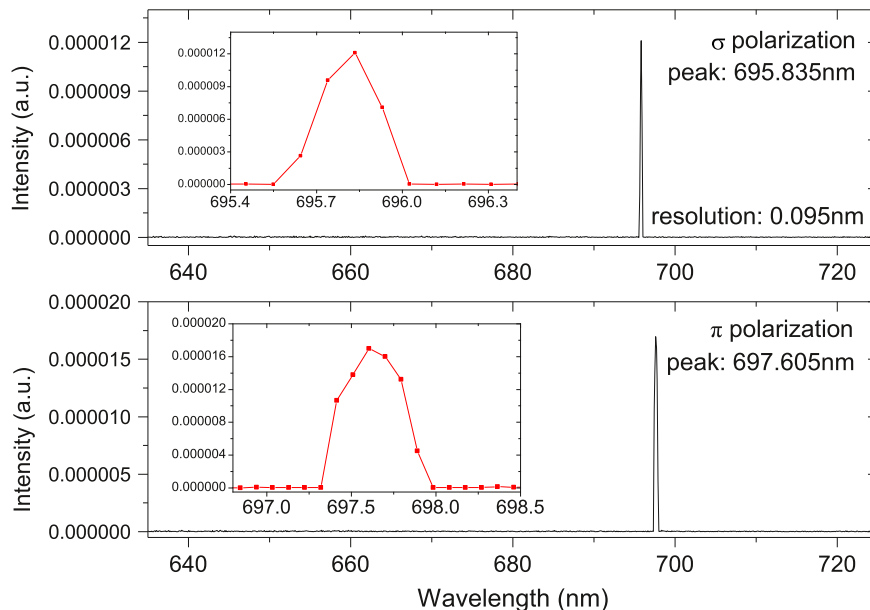
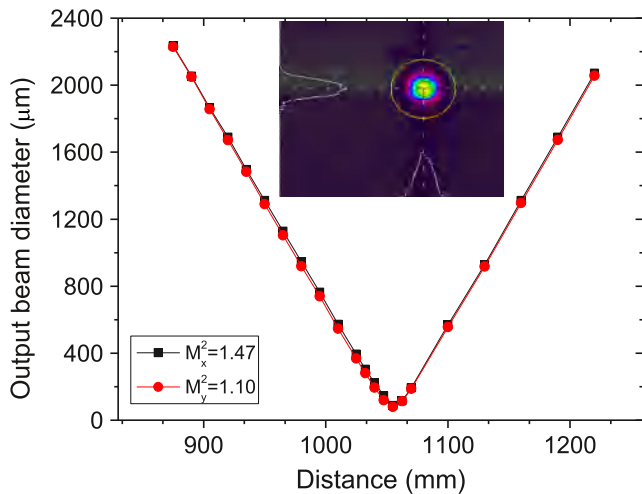


Fig. 4. The laser spectra of the 697.6 and 695.8 nm deep red lasers.



**Fig. 5.**  $x$  and  $y$  diameters of the output laser beam at 695.8 nm as a function of their  $Z$ -axis location.

The FWHM of the two wavelengths was found to be 0.45 and 0.25 nm, respectively. In other words, about 90 and 50 longitudinal modes exist for each case.

To characterize the beam quality of the 695.8 nm deep red laser beam, its diameter was measured in the  $x$  and  $y$  directions at maximum output power (see Fig. 5). The fits of these data then lead to the  $x$  and  $y$   $M^2$  factors  $M_x^2 = 1.47$  and  $M_y^2 = 1.10$ , which clearly shows a good beam quality. It should be noted that in order to achieve a good beam quality of the output laser and to improve the output power realignment of the laser cavity is necessary since the insertion of the etalon at Brewster angle resulted in a transverse mode splitting.

#### 4. Conclusion

In this paper, at first, power scaled operation of  $\pi$ -polarized 697.6 nm laser emission was achieved in a Pr:YLF laser crystal. The pump source emitting blue laser at around 444 nm was an InGaN laser diode with maximum output power up to 2 W instead of commonly used 1-W InGaN laser diode for power scaling. Thus, the  $\pi$ -polarized 697.6 nm laser was generated with maximum output power of 348 mW and slope efficiency of 32.7% with respect to the absorbed pump power. The  $\sigma$ -polarized laser emission at 695.8 nm, orthogonally to the  $\pi$ -polarized 697.6 nm laser, was once obtained using a BBO crystal as birefringence filter. However, in this work, for the first time, we attained the 695.8 nm laser resorting to a simple,

compact and less expensive glass plate placed at Brewster angle acting as birefringence filter. The  $\sigma$ -polarized 695.8 nm laser was power scaled to maximum output power of 116 mW with a slope efficiency of about 18.5%. The beam propagation factor in  $x$  and  $y$  directions were also measured to be  $M_x^2 = 1.47$  and  $M_y^2 = 1.10$ .

#### Acknowledgment

The authors wish to acknowledge the financial support from the National Natural Science Foundation of China (61275050), the Specialized Research Fund for the Doctoral Program of Higher Education (20120121110034, 20130121120043), the Fundamental Research Funds for the Central Universities (2013121022), Natural Science Foundation of Fujian Province of China (2014J01251), and the Scientific Research Foundation for Returned Scholars, Ministry of Education of China.

#### References

- [1] Starecki F, Bolaños W, Braud A, Doualan JL, Brasse G, Benayad A, et al. Red and orange Pr<sup>3+</sup>:YLF planar waveguide laser. *Opt Lett* 2013;38(4):455–7.
- [2] Xu B, Camy P, Doualan JL, Braud A, Cai Z, Balembis F, et al. Frequency doubling and sum-frequency mixing operation at 469.2, 471, and 473 nm in Nd:YAG. *J Opt Soc Am B* 2012;29:346–50.
- [3] Xu B, Camy P, Doualan JL, Cai Z, Moncorgé R. Visible laser operation of Pr<sup>3+</sup>-doped fluoride crystals pumped by a 469 nm blue laser. *Opt Express* 2011;19:1191–7.
- [4] Richter A, Heumann E, Osiać E, Huber G, Seelert W, Diening A. Diode pumping of a continuous-wave Pr<sup>3+</sup>-doped LiYF<sub>4</sub> laser. *Opt Lett* 2004;29:2638–40.
- [5] Hashimoto K, Kannari F. High-power GaN diode-pumped continuous wave Pr<sup>3+</sup>-doped LiYF<sub>4</sub> laser. *Opt Lett* 2007;32:2493–5.
- [6] Fibrich M, Jelinkova H, Sulc J, Nejezchleb K, Skoda V. Diode-pumped Pr:YAP lasers. *Laser Phys Lett* 2011;8(8):559–68.
- [7] Tarallo MG, Poli N, Schioppo M, Sutyryn D, Tino GM. A high-stability semiconductor laser system for a <sup>88</sup>Sr-based optical lattice clock. *Appl Phys B* 2011;103:17–25.
- [8] Liu Zhe, Cai Zhiping, Huang Shunlin, Zeng Chenghang, Meng Zengyou, Bu Yikun, et al. Diode-pumped Pr<sup>3+</sup>:LiYF<sub>4</sub> continuous-wave deep red laser at 698 nm. *J Opt Soc Am B* 2013;30(2):302.
- [9] Liu Zhe, Cai Zhiping, Xu Bin, Zeng Chenghang, Huang Shunlin, Wang Fengjuan, et al. Continuous-wave ultraviolet generation at 349 nm by intracavity frequency doubling of a diode-pumped Pr:LiYF<sub>4</sub> laser. *IEEE Photonics J* 2013;5(4):1500905.
- [10] Liu Zhe, Cai Zhiping, Xu Bin, Huang Shunlin, Zeng Chenghang, Yan Yu, et al. Continuous-wave laser emission of Pr:LiYF<sub>4</sub> at 695.8 nm. *IEEE Photonics Tech Lett* 2014;26(7):675.
- [11] Xu Bin, Liu Zhe, Xu Huiying, Cai Zhiping, Zeng Chenghang, Huang Shunlin, et al. High-efficiency InGaN-LD-pumped bulk Pr:YLF orange laser at 607 nm. *Opt Commun* 2013;305:96–9.
- [12] Pabœuf David, Mhibik Oussama, Bretenaker Fabien, Goldner Philippe, Parisi Daniela, Tonelli Mauro. Diode-pumped Pr:BaY<sub>2</sub>F<sub>8</sub> continuous-wave orange laser. *Opt Lett* 2011;36(2):280.
- [13] Brenier A, Kityk IV. Spectroscopic properties of Pr<sup>3+</sup>-doped Ca<sub>4</sub>GdO(BO<sub>3</sub>)<sub>3</sub> (GdCOB). *J Appl Phys* 2001;90(1):232–6.
- [14] Hegarty J, Huber DL, Yen WM. Fluorescence quenching by cross relaxation in LaF<sub>3</sub>:Pr<sup>3+</sup>. *Phys Rev B* 1982;25:5638.